IEEE Access
Multidisciplinary | Rapid Review | Open Access Journal

Received June 30, 2019, accepted July 12, 2019, date of publication July 16, 2019, date of current version August 7, 2019.

Digital Object Identifier 10.1109/ACCESS.2019.2929094

Fault Diagnosis Method Based on Principal Component Analysis and Broad Learning System

HUIMIN ZHAO[1,3], (Fellow, IEEE), JIANJIE ZHENG[2], (Member, IEEE), JUNJIE XU[1], (Fellow, IEEE), AND WU DENG[1,3,4,5], (Member, IEEE)

[1]College of Electronic Information and Automation, Civil Aviation University of China, Tianjin 300300, China
[2]Software Institute, Dalian Jiaotong University, Dalian 116028, China
[3]The State Key Laboratory of Mechanical Transmissions, Chongqing University, Chongqing 400044, China
[4]Co-Innovation Center of Shandong Colleges and Universities: Future Intelligent Computing, Yantai 264005, China
[5]Traction Power State Key Laboratory, Southwest Jiaotong University, Chengdu 610031, China

Corresponding author: Wu Deng (dw7689@163.com)

This work was supported in part by the National Natural Science Foundation of China under Grant 51605068, Grant 61771087, Grant 51879027, and Grant 51579024, in part by the Open Project Program of State Key Laboratory of Mechanical Transmissions of Chongqing University under Grant SKLMT-KFKT-201803, in part by the Traction Power State Key Laboratory, Southwest Jiaotong University, under Grant TPL1803, in part by the Research Initiation Fund Project of Civil Aviation University of China under Grant 10701004, and in part by the Liaoning BaiQianWan Talents Program.

ABSTRACT Traditional feature extraction methods are used to extract the features of signal to construct the fault feature matrix, which exists the complex structure, higher correlation, and redundancy. This will increase the complex fault classification and seriously affect the accuracy and efficiency of fault identification. In order to solve these problems, a new fault diagnosis (PABSFD) method based on the principal component analysis (PCA) and the broad learning system (BLS) is proposed for rotor system in this paper. In the proposed PABSFD method, the PCA with revealing the signal essence is used to reduce the dimension of the constructed feature matrix and decrease the linear feature correlation between data and eliminate the redundant attributes in order to obtain the low-dimensional feature matrix with retaining the essential features for the classification model. Then, the BLS with low time complexity and high classification accuracy is regarded as a classification model to realize the fault identification; it can efficiently accomplish the fault classification of rotor system. Finally, the actual vibration data of rotor system are selected to test and verify the effectiveness of the PABSFD method. The experimental results show that the PCA method can effectively eliminate the feature correlation and realize the dimension reduction of the feature matrix, the BLS can take on better adaptability, faster computation speed, and higher classification accuracy, and the PABSFD method can efficiently and accurately obtain the fault diagnosis results.

INDEX TERMS Rotor system, fault diagnosis, principal component analysis (PCA), broad learning system (BLS), dimension reduction.

I. INTRODUCTION

Rotor system as the core component of rotating machinery, its running state plays an important role in the safe and stable operation of the equipment. Most of the faults for rotating machinery are caused by rotor system [1]–[3]. Its hazards mainly include noise, rotor instability, and even damaged mechanical structure, which are easy to cause serious accidents [4]–[6]. Therefore, it is of great scientific significance and application value to effectively analyze and diagnose the faults of rotor system [7]–[10].

At present, traditional feature extraction methods for signal of rotor fault mainly include fast Fourier transform (FFT), empirical mode decomposition (EMD), wavelet transform (WT) and so on [11]–[21]. Bouzida *et al.* [22] proposed a fault diagnosis method based on discrete wavelet transform for induction machines. Yang *et al.* [23] proposed a local rub-impact fault diagnosis method based on ensemble local means decomposition. Li *et al.* [24] proposed a fault diagnosis method based on statistical feature extraction and

The associate editor coordinating the review of this manuscript and approving it for publication was Xin Luo.

evaluation method. Cong *et al.* [25] proposed an intelligent detection method using slip matrix construction method based on singular value decomposition for rolling element bearing. Lu *et al.* [26] proposed a novel feature extraction method using adaptive multi-wavelets based on genetic algorithm and the synthetic detection index. Zhang *et al.* [27] proposed an intelligent fault diagnosis method based on support vector machine and ant colony algorithm. Xia *et al.* [28] proposed a novel identification method based on key kernels-PSO for Volterra series identification. Pan *et al.* [29] proposed a new data-driven mono-component identification method based on modified empirical wavelet transform and Hilbert transform. Zheng *et al.* [30] proposed an adaptive parameterless empirical wavelet transform and normalized Hilbert transform for rotor rubbing fault diagnosis. Mishra *et al.* [31] proposed a novel diagnosis scheme based on envelope analysis and wavelet de-noising with sigmoid function based on thresholding to extract the fault related symptoms. Saidi [32] proposed an application of the bispectrum to detect rotor faults in rotating machinery through detection of quadratic phase coupling. An and Zhang [33] proposed a fault diagnosis method based on variational mode decomposition for rotor system with a loose pedestal fault. Li *et al.* [34] proposed an early fault diagnosis method based on differential rational spline-based LMD and Kullback-Leibler divergence. Cheng *et al.* [35] proposed a new fault diagnosis method based on deep learning and Hilbert transform for the drivetrain gearboxes. Yu and He [36] proposed a fault diagnosis method of planetary gearboxes based on data-driven valued characteristic multigranulation model. Chen and Li [37] proposed a fault diagnosis method using PCA and a deep neural network based on stacked denoising autoencoder and the dropout method. Yuan *et al.* [38] proposed a novel fusion diagnosis method based on multi-mode convolutional neural network and t-distributed stochastic neighbor embedding. Lu *et al.* [39] proposed a fast and online order analysis method for permanent magnet synchronous motor bearing fault diagnosis. Zhang *et al.* [40] proposed a feature selection and fault diagnosis framework based on hybrid Filter, Wrapper framework and SVM. Pang *et al.* [41] proposed a novel evaluation index named characteristic frequency band energy entropy to extract the defective features of rotors. Lu *et al.* [42] summarized recent advances in the development of tacholess speed estimation methods for order tracking with its applications to fault diagnosis. Qian *et al.* [43] proposed an edge computing-based method for real-time fault diagnosis and dynamic control of rotating machines. Cheng *et al.* [44] proposed a fault diagnosis method based on a semi-quantitative information model. Yu *et al.* [45] proposed a fault severity identification method of roller bearings using flow graph and non-naive Bayesian inference. The other intelligent methods are proposed in recent year [46]–[56]. They can be applied in the field of fault diagnosis.

However, after the feature extraction of fault signal is reviewed, the formed feature matrix has complex structure, high feature correlation and redundancy. This will increase the complexity of fault classification and reduce the accuracy of fault identification. Therefore, it is crucial to improve the accuracy and efficiency of fault identification. In order to eliminate the redundant information of feature matrix, reduce linear correlation between data, and improve the fault identification efficiency, a simple and efficient dimension reduction method needs to be used in this study. The PCA is a classic dimension reduction method. Because it is simple and easy to understand and the process is completely parameter-free, it has been widely used in various fields, such as image, voice, communication and so on [57]. The essence of the PCA is to calculate the direction of the dimension reduction projection by calculating the covariance matrix of the process data set and then using the feature vector matrix. In addition, the PCA can reveal a simple structure hidden behind complex data, reduce the linear correlation between data, and obtain the best description of the fault state. More importantly, the PCA can reduce the redundancy of fault data under the premise of losing information as little as possible, so as to achieve the purpose of dimension reduction. Therefore, the PCA is used to reduce the dimension of the fault feature matrix in this paper.

Broad learning system(BLS) is an effective and efficient incremental learning system without the need for deep architecture [58]. It is constitutionally designed for fast universal approximation for various applications. In order to realize the fast recognition, the PCA with revealing the signal essence and BLS with low time complexity and high classification accuracy are introduced into fault diagnosis to propose a new fault diagnosis (PABSFD) method for rotor system. In the PABSFD method, the vibration signal is performed by FFT to construct feature matrix, the PCA with revealing the signal essence is used to reduce the dimension of the constructed feature matrix and the linear correlation between data, and eliminate redundant attributes to obtain the low-dimensional matrix with retaining the essential features. Then the BLS is used to regard as a classification model, and the reduced-dimensional feature matrix is input into the BLS model to realize the fault identification. Finally, the actual vibration data is selected to test and verify the effectiveness of the PABSFD method.

II. BASIC METHODS

A. PRINCIPAL COMPONENT ANALYSIS

The PCA is a dimension reduction technique for data [57]. Since it is simple and easy to understand and does not have limitations of parameters, the PCA has been widely applied in all kinds of fields. The main idea of the PCA is to map n-dimensional features to k-dimensional features ($k \leq n$). The k-dimensional features are new orthogonal features, called principal components, which are reconstructed from the original n-dimensional features. The essence of the PCA is to reduce the redundancy of data under the premise of losing information as little as possible, so as to achieve the purpose of dimension reduction.

The steps of the PCA are described in detail as follows:

Step 1: Calculate the sample mean of the n-dimensional data set X, where $X = \{x_1, x_2, \ldots, x_m$.

$$\alpha = \frac{1}{m}\sum_{i=1}^{m} x_i \tag{1}$$

where m is total number of samples, i $= 1, \ldots,$ m, α is the obtained sample mean.

Step 2: Use the generated sample mean to calculate the covariance matrix of the sample set.

$$\mathrm{C} = \frac{1}{m}\sum_{i=1}^{m}(x_i - \alpha)(x_i - \alpha)^T \tag{2}$$

where C is covariance matrix of the sample set.

Step 3: Calculate the feature values and feature vectors of the sample covariance matrix.

$$\mathrm{C} = Q \cdot \sum \cdot Q^T \tag{3}$$

$$\sum = diag(\lambda_1, \lambda_2, \ldots, \lambda_n)\lambda_1 \geq \lambda_2 \geq \cdots \geq \lambda_n \geq 0 \tag{4}$$

$$\mathrm{Q} = [q_1, q_2, \ldots, q_n] \tag{5}$$

where $\sum$ is the arranged diagonal matrix of n feature values of the covariance matrix in descending order, λ_i is the corresponding feature values of covariance matrix, and Q is the feature matrix composed of the corresponding feature vector q_i of the feature value λ_i, i $= 1, \ldots,$ n.

Step 4: Use the obtained feature values and feature vectors to calculate the cumulative variance contribution rate of the first k-row principal elements.

$$\theta = \sum_{i=1}^{k}\lambda_i \Big/ \sum_{j=1}^{m}\lambda_j \tag{6}$$

where θ is cumulative variance contribution rate of the former k-row principal elements, and the value of θ is usually greater than or equal to 0.9. In theory, the value of θ should be as large as possible. From a practical point of the view, the value of θ should be reasonably selected according to the specific solving problem. When the value of θ is reasonably selected, the information of the summarized original sample set of the k-row principal elements can be determined.

Step 5: Realize the dimension reduction using the obtained k-row feature vector.

$$\mathrm{P} = Q_k \tag{7}$$

$$Y = \mathrm{P} \cdot X \tag{8}$$

where P is a feature matrix, which is composed of corresponding feature vectors of the first k-row feature values (k $\leq$ n). Q_k is a feature matrix, which is composed of the first k-row feature values (k $\leq$ n). And Y is the k-dimensional data. The transformation of data set X to Y also realizes the linear transformation of data from n-dimension to k-dimension in order to achieve dimension reduction.

B. BROAD LEARNING SYSTEM

The BLS proposed is built in a flat manner by Professor C. L. Philip Chen. It is design by the idea of using mapping features as a random vector function link neural network (RVFLLNN) input [59]–[61]. The BLS performs feature extraction and dimension reduction for big data by establishing feature nodes and enhancement nodes in order to maintain the validity of the system. In addition, all mapped features and enhancement nodes are directly connected to the output, and the corresponding output coefficients can be obtained by Pseudo, which effectively eliminate the shortcoming of long training time. More importantly, the BLS can also extend the network structure through fast incremental learning without the need of full network retraining. At the same time, when the network is established, the BLS can be combined with a low rank approximation to simplify the system and avoid structural redundancy.

The BLS structure is shown in Figure 1.

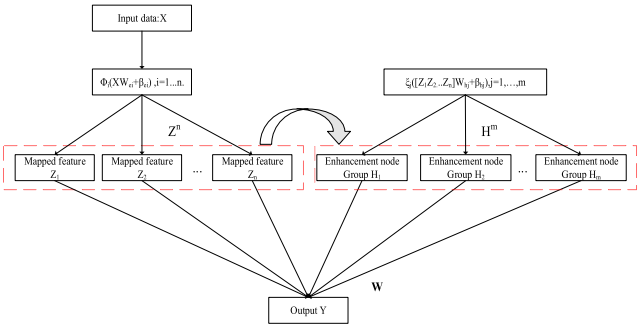

FIGURE 1. The BLS structure.

Assume that we present the input data X and project data φi ($\boldsymbol{X}\boldsymbol{W}e_i + \beta e_i$), which become the ith mapped features $\boldsymbol{Z}i$, where $\boldsymbol{W}e_i$ and βe_i are the random weights with the proper dimensions. Denote $\boldsymbol{Z}^i = [\boldsymbol{Z}_1, \ldots, \boldsymbol{Z}_i]$, which is the concatenation of all the first i groups of mapping features. Similarly, the jth group of enhancement nodes ξ_j ($\boldsymbol{Z}^i\boldsymbol{W}_{hj} + \beta_{hj}$) are denoted as $\boldsymbol{H}_j$, and the concatenation of all the first j groups of enhancement nodes are denoted as $\boldsymbol{H}_j = [\boldsymbol{H}_1, \ldots, \boldsymbol{H}_j]$.

In the BLS, in order to take the advantages of sparse auto-encoder features, the linear inverse problem is applied and the initial $\boldsymbol{W}_{ei}$ is fine-tuned to obtain better features. Assume the input data set $\boldsymbol{X}$, which equips with N samples, each with M dimensions, and $\boldsymbol{Y}$ is the output matrix, which belongs to $R^{N\times C}$. For n feature mappings, each mapping generates k nodes, can be represented as follow.

$$\boldsymbol{Z}i = \varphi(\boldsymbol{X}\boldsymbol{W}e_i + \beta e_i), \quad i = 1, \ldots, n \tag{9}$$

where $\boldsymbol{W}e_i$ and βe_i are randomly generated. Denote all feature nodes is $\boldsymbol{Z}^n \equiv [\boldsymbol{Z}1, \ldots, \boldsymbol{Z}n]$, and the mth group of enhancement nodes is denoted as follow.

$$\boldsymbol{H}m \equiv \xi(\boldsymbol{Z}n\boldsymbol{W}hm + \beta hm) \tag{10}$$

Hence, the BLS can be represented as follow.

$$\begin{aligned} \boldsymbol{Y} &= [\boldsymbol{Z}_1, \ldots, \boldsymbol{Z}_n | \xi(\boldsymbol{Z}_n \boldsymbol{W}_{h1} + \beta_{h1}), \ldots, \xi(\boldsymbol{Z}_n \boldsymbol{W}_{hm} + \beta_{hm})] \boldsymbol{W}_m \\ &= [\boldsymbol{Z}_1, \ldots, \boldsymbol{Z}_n | \boldsymbol{H}_1, \ldots, \boldsymbol{H}_m] \boldsymbol{W}^m \\ &= [\boldsymbol{Z}^n | \boldsymbol{H}^m] \boldsymbol{W}^m \end{aligned} \tag{11}$$

where the $\boldsymbol{W}^m = [\boldsymbol{Z}^n | \boldsymbol{H}^m]^+ \boldsymbol{Y}$.

The steps of the BLS is described as follows:

Step 1: The input data is linearly transformed to form a feature node of the BLS.

Step 2: The feature node randomly generates an enhancement node through nonlinear transformation.

Step 3: All mapping features and enhancement nodes are directly connected to the output.

Step 4: The weights of corresponding output can be obtained by Pseudo. After the output weight is obtained, the BLS is constructed.

III. FAULT DIAGNOSIS METHOD BASED ON PCA AND BLS

A. A NEW FAULT DIAGNOSIS METHOD

The rotor system is the core component of rotating machine, and its operating state determines the working state. Therefore, the effective identification fault of rotor system has important scientific significance and application value. At present, for the fault data, the obtained feature matrix has complex structure, high feature correlation and redundancy, which will affect the performance of the classification model. Therefore, in order to eliminate the redundancy of feature matrix and improve the accuracy of fault classification, the PCA and BLS are introduced into fault diagnosis to propose a new fault diagnosis(PABSFD) method. In the proposed PABSFD method, the vibration signal is performed by FFT to construct feature matrix, then the PCA is used to reduce the dimension of the constructed feature matrix and decrease the linear correlation between data, and eliminate redundant attributes in order to obtain the low-dimensional feature matrix with retaining the essential features. Next, in the BLS, the feature nodes and the enhancement nodes can implement feature extraction and dimension reduction. At the same time, all nodes of the BLS model are directly connected to the output, and the corresponding output coefficients by Pseudo can be obtained, which can greatly shorten the computing time. The BLS is used to regard as a classification model, and the reduced-dimensional feature matrix is input into the BLS model in order to realize the fault identification. The proposed PABSFD method can efficiently accomplish the fault diagnosis for rotor system. And it has higher diagnosis accuracy and lower time complexity.

B. FAULT DIAGNOSIS MODEL

In the PABSFD method, the fault vibration signal of rotor system is collected, and the FFT is used to process the fault vibration signal to construct the fault feature matrix. Then the PCA is used to reduce the dimension of feature matrix, and the BLS is used to classify the reduced-dimensional features. The proposed PABSFD method can reduce the redundancy of fault features, shorten the classification time, and improve the efficiency of fault identification. The flow of the PABSFD method is shown in Figure 2.

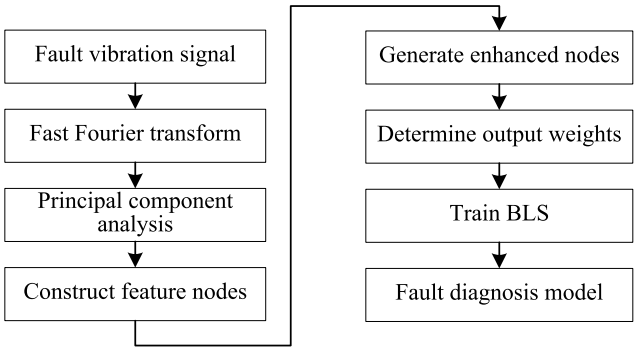

FIGURE 2. The flow of the PABSFD method.

The specific steps of the PABSFD method are described as follows:

Step 1: The FFT is used to deal with the fault vibration signal in order to transform the vibration signal from time domain to frequency domain.

Step 2: Select initial parameters for the PABSFD method, including the number of feature nodes and enhancement nodes, regularization parameter, node scaling scale value, and so on.

Step 3: Reasonably select the cumulative variance contribution rate to achieve dimension reduction using the PCA method.

Step 4: Construct a feature node by reducing the dimensioned data.

Step 5: Generate an enhancement node according to the feature nodes.

Step 6: Generate the output weights of the BLS to complete the construction of the BLS model and obtain an ideal classification model.

Step 7: Test effectiveness of the PABSFD model by the test sample.

Step 8: Fault diagnosis results are obtained and output.

IV. EXPERIMENT AND ANALYSIS

A. EXPERIMENT DATA AND ENVIRONMENT

In order to verify the effectiveness of the proposed PABSFD method, the QPZZ-II rotary machinery experiment platform is used to obtain experiment data in here. The experiment platform can simulate many kinds of fault states of rotating machinery. The fault vibration signals are collected under different rotating speeds. The shift range is 75-1450 r/min. The experiment platform is shown in Figure 3.

The experiment uses the USB-4431 data acquisition card, vibration acceleration sensor and LabVIEW software produced by National Instruments of the United States for vibration signal acquisition. The sampling frequency is 12kHz and the sampling time is 100s. The rotating speed of motor is 1000r/min, 1250r/min and 1500r/min, respectively. Nine kinds of fault vibration signals and one normal vibration

TABLE 1. Description of the fault type.

Fault type	Name	Fault classification
Inner ring	IR	1
Outer ring	OR	2
Rolling element	Ball	3
Outer ring + Rolling element	OUTB	4
Rotor unbalance	ROTOR	5
Rotor unbalance + Inner ring	ROIN	6
Rotor unbalance + Outer ring	ROOUT	7
Rotor unbalance +Rolling element	ROB	8
Rotor unbalance + Outer ring + Rolling element	ROOB	9
Normal	NORMAL	10

TABLE 2. Comparison of various dimension reduction methods (1000r/min).

Methods	Training time(s)	Training accuracy (%)	Test time (s)	Test accuracy(%)	Variance
BLSFD(-)	1.695	100	0.198	99.91	0.043
LEBSFD(LLE)	1.358	99.51	0.153	99.14	0.042
LABSFD(LTSA)	**1.104**	77.69	0.162	69.73	0.312
LLSABSFD(LLTSA)	1.251	99.96	0.157	99.12	0.034
PABSFD(**PCA**)	**1.190**	**99.98**	**0.161**	**99.95**	0.024

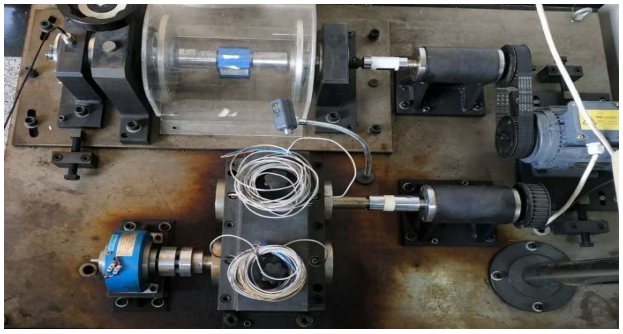

FIGURE 3. The experiment platform of QPZZ-II.

signal are collected under no-load. The intercept length of vibration signal is 1024. The fault types and classification label are shown in Table 1. The experiments were performed on a computer equipped with an Intel(R) Xeon(R) Bronze 3104 CPU @ 1.70GHz, 16GB memory on the MATLAB 2018b software platform.

The vibration signal under different rotating speeds were divided into the same data, that is, 936 sets of data were used as training samples and 234 sets of data were used as test samples. Among these data, each set contains all vibration signals in Table 1.

The FFT is used to transform the collected vibration signals from time domain to frequency domain in order to construct feature matrix. After the FFT transformation is realized, the length of data is changed from 1024 to 512.

B. COMPARISON AND ANALYSIS RESULTS OF DIMENSION REDUCTION

In order to test the effectiveness of the PCA method, the PABSFD based on PCA and BLS is compared with other dimension reduction methods, including the BLSFD based on BLS, LEBSFD based on local linear embedding (LLE) and BLS, LABSFD based on local tangent spatial alignment (LTSA) and BLS, LLSABSFD based on linear local tangent spatial alignment (LLTSA) and BLS. After the data is reduced by different methods, the dimensions are kept at 150 dimensions. At the same time, the BLS model is used to classify the data of the dimension reduction. The structure of BLS model (feature node-enhancement node) is 500-500. In addition, the experimental results are obtained after 10 times. The experiment results under 1000r/min, 1250r/min, and 1500r/min are shown in Tables 2, 3, and 4, respectively.

As can be seen from Table 2, for rotating speed of 1000r/min, compared with the data without dimension reduction, these dimension reduction methods are used to reduce the dimension of data, and all dimension-reduced data can effectively reduce the training time and test time. Especially for dimension-reduced data using the PCA method, the test accuracy is **99.95%** and the variance is **0.024**. The results are best in these methods. Therefore, the experiment results show that the PCA method takes on better ability of dimension reduction. And it can maintain extremely high stability, which is superior to other dimension reduction methods.

As can be seen from Table 3, for rotating speed of 1250r/min, although the dimension-reduced data using LTSA can effectively improve the training time, the test accuracy is lower value. This indicates that the LTSA method is not ideal. For dimension-reduced data using the PCA method, the training accuracy and test accuracy are 100% and the variance is 0. The experiment results are better than 99.93% and 99.87% of LLTSA. At the same time, the PCA method can also speed up the training time and test time. Compared

TABLE 3. Comparison of various dimension reduction methods (1250r/min).

Methods	Training time(s)	Training accuracy (%)	Test time (s)	Test accuracy(%)	Variance
BLSFD(-)	1.963	100	0.218	99.95	0.0274
LEBSFD(LLE)	1.297	99.61	0.152	99.18	0.0270
LABSFD(LTSA)	**1.036**	87.84	0.138	84.31	0.0493
LLSABSFD(LLTSA)	1.802	99.93	0.179	99.87	0.0247
PABSFD(**PCA**)	**1.330**	100	**0.142**	100	0

TABLE 4. Comparison of various dimension reduction methods (1500r/min).

Methods	Training time(s)	Training accuracy (%)	Test time (s)	Test accuracy(%)	Variance
BLSFD(-)	1.684	100	0.212	99.95	0.037
LEBSFD(LLE)	1.472	99.51	0.165	99.41	0.027
LABSFD(LTSA)	**1.026**	77.77	0.135	69.52	0.054
LLSABSFD(LLTSA)	1.211	99.72	0.142	99.62	0.043
PABSFD(PCA)	1.179	**99.98**	**0.138**	**99.97**	0.024

with the data without dimension reduction, the dimension-reduced data using the PCA method can effectively reduce the training time and test time, and improve the stability of the PABSFD method. The experiment results show that the PCA method has better dimension reduction effect and the PABSFD method takes on best diagnosis accuracy.

As can be seen from Table 4, for rotating speed of 1500r/min, the obtained training accuracy and test accuracy for dimension-reduced data using the PCA method are 99.98% and 99.97%, respectively. The test accuracy is best in these methods. In addition, the variance using the PCA method is **0.024**, which show that the PCA method is also superior to several other reduction methods in the stability. Compared with the data without dimension reduction, the dimension-reduced data using the PCA method can reduce the training time and test time, and improve the test accuracy and stability. The experiment results show that the PCA method takes on better the ability of dimension reduction.

In summary, the dimension-reduced data using all reduction methods can reduce training time and test time. However, it can find that the dimension-reduced data using the PCA method can better improve the test accuracy and stability. This shows that the PCA method can better remove data redundancy and preserve the validity of the data. In addition, the PCA method can improve the classification efficiency of the BLS model.

C. COMPARISON AND ANALYSIS OF CUMULATIVE CONTRIBUTION RATES OF PRINCIPAL COMPONENTS

In order to analyze the influence of the cumulative variance contribution rate on the classification effect, in this experiment, the classifier of the BLS is used in here, and the structure (feature node-enhancement node) of BLS is set to 500-500. The initial cumulative variance contribution rate is set 0.95, which is increases by 0.005 for each time, up to 0.995.

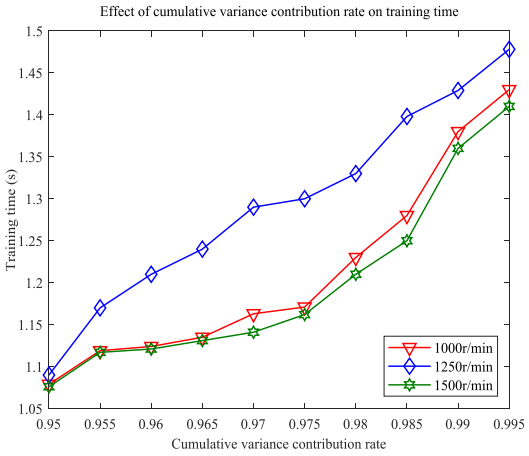

FIGURE 4. Influence of cumulative variance contribution rate on training time.

The experiment comparison includes the test accuracy and training time. At the same time, the experiment results are obtained after average value for 10 times. The experiment results are shown in Figure 4 and Figure 5.

As can be seen from Figure 4, the training time of all data will increase significantly with the increasing of the cumulative variance contribution rate. This is because the cumulative variance contribution rate is higher, the PCA method has less dimension reduction for data, the training time of the BLS is longer.

As can be seen from Figure 5, within a certain range, with the increasing of the cumulative variance contribution rate, the test accuracy under different speeds takes on the trend of increasing first and then stabilizing. The cumulative variance contribution rate of the test accuracy is 0.98 under 1000r/min and 1500r/min, and the cumulative variance contribution rate of the test accuracy is 0.965 under 1250/min. The cumulative variance contribution rate of the test accuracy under 1250/min is lower than that under other two speeds. The results show that the cumulative variance contribution rate is different for

TABLE 5. Classification comparison of datasets after PCA (1000r/min).

Methods	Training time(s)	Training accuracy (%)	Test time (s)	Test accuracy (%)	Variance
PAEMFD(ELM)	13.01	99.94	0.281	99.87	**0**
PAHMFD(HELM)	1.210	99.79	0.169	99.71	0.017
PARMFD(RELM)	2.160	**99.98**	0.174	99.88	0.015
PABSFD(BLS)	**1.190**	**99.98**	**0.161**	**99.95**	0.024

TABLE 6. Classification comparison of data sets after PCA (1250r/min).

Methods	Training time(s)	Training accuracy (%)	Test time (s)	Test accuracy (%)	Variance
PAEMFD(ELM)	12.10	100	0.312	100	0
PAHMFD(HELM)	1.410	100	0.145	100	0
PARMFD(RELM)	2.120	100	0.148	100	0
PABSFD(BLS)	**1.330**	100	**0.142**	100	0

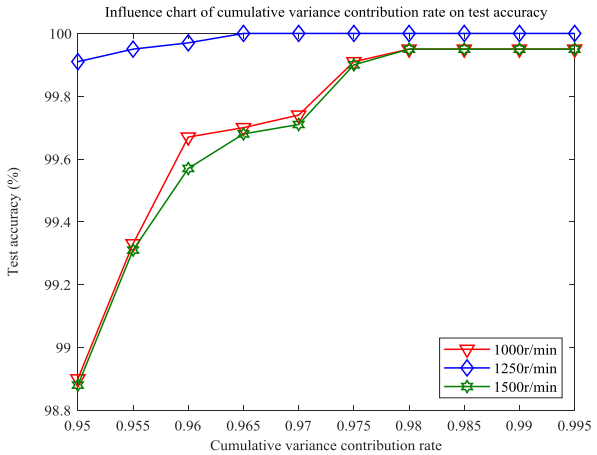

FIGURE 5. Influence of cumulative variance contribution rate on test accuracy.

the data under different working conditions. The experiment results show that the PCA method can reduce the redundancy of data under different speeds. Therefore, the cumulative variance contribution rate can be flexibly selected for the specific data under different working conditions in order to reasonably and effectively extract the fault features.

In summary, with the increasing of the cumulative variance contribution rate, the test accuracy of three kinds of data takes on the trend of increasing first and then stabilizing, but the required time of modeling takes on a continuous increasing. This shows that the PCA method can effectively preserve data features and reduce the required time of modeling for three kinds of data.

D. COMPARISON AND ANALYSIS OF CLASSIFICATION MODELS

In order to prove the effectiveness of the PABSFD based on PCA and BLS, the PAEMFD based on PCA and extreme learning machine (ELM), the PAHMFD based on PCA and multilayer extreme learning machine (HELM), the PARMFD based on PCA and regularized extreme learning machine (RELM) are selected in here. Among them, the number of hidden layer nodes of the ELM is set as1000, the structure of the HELM is set as 100-100-1000, the number of nodes of the RELM is set as 1000, and the number of nodes of the BLS is set as 500-500. The activation function selects the Sigmoid function for the hidden layer of the ELM, HELM, and RELM, and the activation function also selects the Sigmoid function for the enhancement layer of BLS. At the same time, the weights and offsets of the feature node layer and the enhancement node layer in the BLS are extracted from the standard uniform distribution on the interval $[-1, 1]$. In addition, the experiment results are described in detail by the obtained average values of 10 times for each method.

The experimental results at 1000r/min, 1250r/min, and 1500r/min are shown in Tables 5, 6, and 7, respectively.

As can be seen from Table 5, for rotating speed of 1000r/min, the ELM shows great stability during the training and test, but its training time and test time are much more than other classification models. The training accuracy and test accuracy are 99.98% and 99.95%, respectively. Therefore, the BLS model is superior to other classifiers in training accuracy and test accuracy. At the same time, the training time of the BLS model only needs 1.19s, which is better than training times of the ELM, RELM, HELM. The experiment results show that the BLS can better complete the task of fault classification.

As can be seen from Table 6, for rotating speed of 1250r/min and the dimension-reduced data using the PCA method, all classification models can obtain the optimal training accuracy and test accuracy, and the test accuracy maintains extremely high stability. This also proves that the PCA method is extremely stable. From the perspective of time, the training time and test time of the BLS only needs 1.33s and 1.42s, respectively. Therefore, the time complexity is lower than those of ELM, HELM and RELM. The experiment results show that the BLS is competitive with other classification models and the PABSFD method takes on better fault diagnosis accuracy.

TABLE 7. Classification comparison of datasets after PCA (1500r/min).

Methods	Training time(s)	Training accuracy (%)	Test time (s)	Test accuracy (%)	Variance
PAEMFD(ELM)	12.06	99.96	0.218	99.87	**0**
PAHMFD(HELM)	1.337	99.73	0.162	99.41	**0**
PARMFD(RELM)	2.110	99.78	0.148	99.93	**0**
PABSFD(BLS)	**1.179**	**99.98**	**0.138**	**99.97**	0.024

As can be seen from Table 7, for rotating speed of 1500r/min, the HELM and RELM can faster realize the fault diagnosis. At the same time, the HELM and RELM can maintain excellent stability. When the BLS model is applied to classify the faults, the training accuracy and test accuracy are 99.98% and 99.97%, respectively. The accuracy is better than other classification models. From the perspective of training time, the training time of the BLS model is the shortest, which only need 1/10 training time of the ELM. The experiment results show that the BLS model can efficiently realize fault classification. And the PABSFD method can obtain high diagnosis accuracy.

In summary, for BLS classification model, the test time under1500r/min is shorter than the test time under 1000r/min and 1250r/min. The test time under1250r/min is shorter than the test time under 1000r/min. This means that the rotating speed is faster, the test time is shorter for fault diagnosis of the collected data. For the fault data under different speeds, compared with the ELM, HELM and RELM, the BLS can fastest complete the classification, it can realize the fault diagnosis with the best test accuracy under different fault data. Therefore, the test accuracy and test time of the BLS model are best than other comparison methods, and the stability of the BLS model is similar to the stabilities of the ELM, HELM and RELM. In addition, the experiment results show that the BLS model takes on stronger generalization ability.

V. CONCLUSION

In this paper, a new fault diagnosis(PABSFD) method based on the PCA and BLS is proposed. Firstly, the FFT is used to transform the vibration signal from time domain to frequency domain. Then the PCA method is used to reduce the dimension of the constructed feature matrix and decrease the linear correlation between data in order to form the low-dimensional feature matrix. And the reduced feature vector is input into the BLS model in order to obtain a new fault classification model for realizing the purpose of fault diagnosis. The main conclusions are summarized as follows:

(1) The dimension reduction method of PCA can effectively eliminate the correlation of feature vectors in the feature matrix and realize the dimension reduction of the feature matrix, so as to reduce the redundancy of the feature matrix.

(2) In practical applications, the PCA method can select the cumulative variance contribution rate according to the specific solving problem in order to reasonably reduce the dimension of the feature matrix, which reflects the flexibility.

(3) The BLS performs feature extraction and dimension reduction by establishing feature nodes and enhancement nodes in order to maintain the validity of the system. The BLS model is introduced into the field of fault diagnosis and can broaden its applicability.

(4) Compared with other classification models, the PABSFD method can efficiently realize fault diagnosis. The experiment results show that the BLS model takes on good superiority. And for multi-classification problems under different speeds, the PABSFD method takes on good adaptability and strong stability.

REFERENCES

[1] J. P. Jing and G. Meng, "A novel method for multi-fault diagnosis of rotor system," *Mech. Mach. Theory*, vol. 44, no. 4, pp. 697–709, Apr. 2009.

[2] W. Deng, R. Yao, H. Zhao, X. Yang, and G. Li, "A novel intelligent diagnosis method using optimal LS-SVM with improved PSO algorithm," *Soft Comput.*, vol. 23, no. 7, pp. 2445–2462, Apr. 2019.

[3] J. Guo, Y. Mu, M. Xiong, Y. Liu, and J. Gu, "Activity feature solving based on TF-IDF for activity recognition in smart homes," *Complexity*, vol. 2019, Mar. 2019, Art. no. 5245373. doi: 10.1155/2019/5245373.

[4] S. Lu, Q. He, and J. Wang, "A review of stochastic resonance in rotating machine fault detection," *Mech. Syst. Signal Process.*, vol. 116, pp. 230–260, Feb. 2019.

[5] H. Jiang, C. Li, and H. Li, "An improved EEMD with multiwavelet packet for rotating machinery multi-fault diagnosis," *Mech. Syst. Signal Process.*, vol. 36, no. 2, pp. 225–239, 2013.

[6] H. Chen, Y. Xu, M. Wang, and X. Zhao, "A balanced whale optimization algorithm for constrained engineering design problems," *Appl. Math. Model.*, vol. 71, pp. 45–59, Jul. 2019.

[7] H. M. Zhao, M. Sun, W. Deng, and X. Yang, "A new feature extraction method based on EEMD and multi-scale fuzzy entropy for motor bearing," *Entropy*, vol. 19, no. 1, p. 14, 2017.

[8] Z. Ren, R. Skjetne, Z. Jiang, Z. Gao, and A. S. Verma, "Integrated GNSS/IMU hub motion estimator for offshore wind turbine blade installation," *Mech. Syst. Signal Process.*, vol. 123, pp. 222–243, May 2019.

[9] S. Lu, P. Zheng, Y. Liu, Z. Cao, H. Yang, and Q. Wang, "Sound-aided vibration weak signal enhancement for bearing fault detection by using adaptive stochastic resonance," *J. Sound Vib.*, vol. 449, pp. 18–29, Jun. 2019.

[10] H. M. Zhao, R. Yao, L. Xu, Y. Yuan, G. Y. Li, and W. Deng, "Study on a novel fault damage degree identification method using high-order differential mathematical morphology gradient spectrum entropy," *Entropy*, vol. 20, no. 9, p. 682, 2018.

[11] W. Deng, H. Zhao, L. Zou, G. Li, X. Yang, and D. Wu, "A novel collaborative optimization algorithm in solving complex optimization problems," *Soft Comput.*, vol. 21, no. 15, pp. 4387–4398, Aug. 2017.

[12] Y. Q. Liu, X. K. Yi, Z. G. Zhai, and J. X. Gu, "Feature extraction based on information gain and sequential pattern for English question classification," *IET Softw.*, vol. 12, no. 6, pp. 520–526, 2018.

[13] S. K. Guo, R. Chen, H. Li, T. L. Zhang, and Y. Q. Liu, "Identify severity bug report with distribution imbalance by CR-SMOTE and ELM," *Int. J. Softw. Eng. Knowl. Eng.*, vol. 29, no. 6, pp. 139–175, 2019.

[14] J. Luo, H. Chen, Q. Zhang, Y. Xu, H. Huang, and X. Zhao, "An improved grasshopper optimization algorithm with application to financial stress prediction," *Appl. Math. Model.*, vol. 64, pp. 654–668, Dec. 2018.

[15] W. Deng, J. Xu, and H. Zhao, "An improved ant colony optimization algorithm based on hybrid strategies for scheduling problem," *IEEE Access*, vol. 7, pp. 20281–20292, 2019

[16] Z. R. Ren, R. Skjetne, and Z. Gao, "A crane overload protection controller for blade lifting operation based on model predictive control," *Energies*, vol. 12, no. 1, p. 50, 2019.

[17] Y. R. Zhou, T. Li, J. Shi, and Z. Qian, "A CEEMDAN and XGBOOST-based approach to forecast crude oil prices," *Complexity*, vol. 2019, Jan. 2019, Art. no. 4392785.

[18] W. Deng, H. Zhao, X. Yang, J. Xiong, M. Sun, and B. Li, "Study on an improved adaptive PSO algorithm for solving multi-objective gate assignment," *Appl. Soft Comput.*, vol. 59, pp. 288–302, Oct. 2017.

[19] Y. Liu, X. Wang, Z. Zhai, R. Chen, B. Zhang, and Y. Jiang, "Timely daily activity recognition from headmost sensor events," *ISA Trans.*, to be published. doi: 10.1016/j.isatra.2019.04.026.

[20] R. Chen, S. Guo, X. Wang, and T. Zhang, "Fusion of multi-RSMOTE with fuzzy integral to classify bug reports with an imbalanced distribution," *IEEE Trans. Fuzzy Syst.*, to be published. doi: 10.1109/TFUZZ.2019.2899809.

[21] W. Deng, S. Zhang, H. Zhao, and X. Yang, "A novel fault diagnosis method based on integrating empirical wavelet transform and fuzzy entropy for motor bearing," *IEEE Access*, vol. 6, pp. 35042–35056, 2019.

[22] A. Bouzida, O. Touhami, R. Ibtiouen, A. Belouchrani, M. Fadel, and A. Rezzoug, "Fault diagnosis in industrial induction machines through discrete wavelet transform," *IEEE Trans. Ind. Electron.*, vol. 58, no. 9, pp. 4385–4395, Sep. 2011.

[23] Y. Yang, J. Cheng, and K. Zhang, "An ensemble local means decomposition method and its application to local rub-impact fault diagnosis of the rotor systems," *Measurement*, vol. 45, no. 3, pp. 561–570, Apr. 2012.

[24] W. Li, Z. Zhu, F. Jiang, G. Zhou, and G. Chen, "Fault diagnosis of rotating machinery with a novel statistical feature extraction and evaluation method," *Mech. Syst. Signal Process.*, vols. 50–51, pp. 414–426, Jan. 2015.

[25] F. Y. Cong, W. Zhong, S. Tong, N. Tang, and J. Chen, "Research of singular value decomposition based on slip matrix for rolling bearing fault diagnosis," *J. Sound Vib.*, vol. 344, pp. 447–463, May 2015.

[26] N. Lu, H. Xiao, and O. P. Malik, "Feature extraction using adaptive multiwavelets and synthetic detection index for rotor fault diagnosis of rotating machinery," *Mech. Syst. Signal Process.*, vols. 52–53, pp. 393–415, Feb. 2015.

[27] X. Zhang, W. Chen, B. Wang, and X. Chen, "Intelligent fault diagnosis of rotating machinery using support vector machine with ant colony algorithm for synchronous feature selection and parameter optimization," *Neurocomputing*, vol. 167, pp. 260–279, Nov. 2015.

[28] X. Xia, J. Zhou, J. Xiao, and H. Xiao, "A novel identification method of Volterra series in rotor-bearing system for fault diagnosis," *Mech. Syst. Signal Process.*, vols. 66–67, pp. 557–567, Jan. 2016.

[29] J. Pan, J. Chen, Y. Zi, J. Yuan, B. Chen, and Z. He, "Data-driven monocomponent feature identification via modified nonlocal means and MEWT for mechanical drivetrain fault diagnosis," *Mech. Syst. Signal Process.*, vol. 80, pp. 533–552, Dec. 2016.

[30] J. Zheng, H. Pan, S. Yang, and J. Cheng, "Adaptive parameterless empirical wavelet transform based time-frequency analysis method and its application to rotor rubbing fault diagnosis," *Signal Process.*, vol. 130, pp. 305–314, Jan. 2017.

[31] C. Mishra, A. K. Samantaray, and G. Chakraborty, "Rolling element bearing fault diagnosis under slow speed operation using wavelet de-noising," *Measurement*, vol. 103, pp. 77–86, Jun. 2017.

[32] L. Saidi, "The deterministic bispectrum of coupled harmonic random signals and its application to rotor faults diagnosis considering noise immunity," *Appl. Acoust.*, vol. 122, pp. 72–87, Jul. 2017.

[33] X. An and F. Zhang, "Pedestal looseness fault diagnosis in a rotating machine based on variational mode decomposition," *Proc. Inst. Mech. Eng., C, J. Mech. Eng. Sci.*, vol. 231, no. 13, pp. 2493–2502, Jul. 2017.

[34] Y. Li, X. Liang, Y. Yang, M. Xu, and W. Huang, "Early fault diagnosis of rotating machinery by combining differential rational spline-based LMD and K–L divergence," *IEEE Trans. Instrum. Meas.*, vol. 66, no. 11, pp. 3077–3090, Nov. 2017.

[35] F. Cheng, J. Wang, L. Qu, and W. Qiao, "Rotor-current-based fault diagnosis for DFIG wind turbine drivetrain gearboxes using frequency analysis and a deep classifier," *IEEE Trans. Ind. Appl.*, vol. 54, no. 2, pp. 1062–1071, Mar./Apr. 2018.

[36] J. Yu and Y. He, "Planetary gearbox fault diagnosis based on data-driven valued characteristic multigranulation model with incomplete diagnostic information," *J. Sound Vib.*, vol. 429, pp. 63–77, Sep. 2018.

[37] Z. Chen and Z. Li, "Fault diagnosis method of rotating machinery based on stacked denoising autoencoder," *J. Intell. Fuzzy Syst.*, vol. 34, no. 6, pp. 3443–3449, Jun. 2018.

[38] Z. Yuan, L. Zhang and L. Duan, "A novel fusion diagnosis method for rotor system fault based on deep learning and multi-sourced heterogeneous monitoring data," *Meas. Sci. Technol.*, vol. 29, no. 11, Art. no. 115005, Oct. 2018.

[39] S. Lu, Q. He, and J. Zhao, "Bearing fault diagnosis of a permanent magnet synchronous motor via a fast and online order analysis method in an embedded system," *Mech. Syst. Signal Process.*, vol. 113, pp. 36–49, Dec. 2018.

[40] X. Zhang, Q. Zhang, M. Chen, Y. Sun, X. Qin, and H. Li, "A two-stage feature selection and intelligent fault diagnosis method for rotating machinery using hybrid filter and wrapper method," *Neurocomputing*, vol. 275, pp. 2426–2439, Jan. 2018.

[41] B. Pang, G. Tang, C. Zhou, and T. Tian, "Rotor fault diagnosis based on characteristic frequency band energy entropy and support vector machine," *Entropy*, vol. 20, no. 12, p. 932, Dec. 2018.

[42] S. Lu, R. Yan, Y. Liu, and Q. Wang, "Tacholess speed estimation in order tracking: A review with application to rotating machine fault diagnosis," *IEEE Trans. Instrum. Meas.*, vol. 68, no. 7, pp. 2315–2332, Jul. 2019. doi: 10.1109/TIM.2019.2902806.

[43] G. Qian, S. Lu, D. Pan, H. Tang, Y. Liu, and Q. Wang, "Edge computing: A promising framework for real-time fault diagnosis and dynamic control of rotating machines using multi-sensor data," *IEEE Sensors J.*, vol. 19, no. 11, pp. 4211–4220, Jun. 2019. doi: 10.1109/JSEN.2019.2899396.

[44] C. Cheng, X. Qiao, H. Luo, W. Teng, M. Gao, B. Zhang, and X. Yin, "A semi-quantitative information based fault diagnosis method for the running gears system of high-speed trains," *IEEE Access*, vol. 7, pp. 38168–38178, 2019.

[45] J. Yu, Y. Xu, G. Yu, and L. Liu, "Fault severity identification of roller bearings using flow graph and non-naive Bayesian inference," *Proc. Inst. Mech. Eng., C, J. Mech. Eng. Sci.*, vol. 233, no. 14, pp. 5161–5171, Jan. 2019. doi: 10.1177/0954406219834966.

[46] T. Li, Z. Hu, Y. Jia, J. Wu, and Y. Zhou, "Forecasting crude oil prices using ensemble empirical mode decomposition and sparse Bayesian learning," *Energies*, vol. 11, no. 7, p. 1882, Jul. 2018.

[47] Y. T. Xu, H. Chen, A. A. Heidari, J. Luo, Q. Zhang, X. Zhao, and C. Li, "An efficient chaotic mutative moth-flame-inspired optimizer for global optimization tasks," *Expert Syst. Appl.*, vol. 129, pp. 135–155, Sep. 2019.

[48] F. Sun, Y. Yao, G. Li, and W. Liu, "Simulation of real gas mixture transport through aqueous nanopores during the depressurization process considering stress sensitivity," *J. Petroleum Sci. Eng.*, vol. 178, pp. 829–837, Jul. 2019.

[49] S. Guo, Y. Liu, R. Chen, X. Sun, and X. Wang, "Improved SMOTE algorithm to deal with imbalanced activity classes in smart homes," *Neural Process Lett.*, to be published. doi: 10.1007/s11063-018-9940-3.

[50] G. Liu, B. Chen, S. Jiang, H. Fu, L. Wang, and W. Jiang, "Double entropy joint distribution function and its application in calculation of design wave height," *Entropy*, vol. 21, no. 1, p. 64, Jan. 2019.

[51] T. Li, J. Shi, X. Li, J. Wu, and F. Pan, "Image encryption based on pixel-level diffusion with dynamic filtering and DNA-level permutation with 3D Latin cubes," *Entropy*, vol. 21, no. 3, p. 319, Mar. 2019.

[52] H. Fu, G. Manogaran, K. Wu, M. Cao, S. Jiang, and A. Yang, "Intelligent decision-making of online shopping behavior based on Internet of Things," *Int. J. Inf. Manage.*, to be published. doi: 10.1016/j.ijinfomgt.2019.03.010.

[53] F. Sun, Y. Yao, G. Li, and M. Dong, "Transport behaviors of real gas mixture through nanopores of shale reservoir," *J. Petroleum Sci. Eng.*, vol. 177, pp. 1134–1141, Jun. 2019.

[54] Y. Xu, H. Chen, J. Luo, Q. Zhang, S. Jiao, and X. Zhang, "Enhanced moth-flame optimizer with mutation strategy for global optimization," *Inf. Sci.*, vol. 492, pp. 181–203, Aug. 2019.

[55] S. Guo, R. Chen, M. Wei, H. Li, and Y. Liu, "Ensemble data reduction techniques and multi-RSMOTE via fuzzy integral for bug report classification," *IEEE Access*, vol. 6, pp. 5934–45950, 2018.

[56] G. Liu, Z. Gao, B. Chen, H. Fu, S. Jiang, L. Wang, and Y. Kou, "Study on threshold selection methods in calculation of ocean environmental design parameters," *IEEE Access*, vol. 7, pp. 39515–39527, 2019.

[57] H. Van Luong, N. Deligiannis, J. Seiler, S. Forchhammer, and A. Kaup, "Compressive online robust principal component analysis via n-ℓ_1 minimization," *IEEE Trans. Image Process.*, vol. 27, no. 9, pp. 4314–4329, Sep. 2018.

[58] C. L. P. Chen, Z. Liu, and S. Feng, "Universal approximation capability of broad learning system and its structural variations," *IEEE Trans. Neural Netw. Learn. Syst.*, vol. 30, no. 4, pp. 1191–1204, Apr. 2018. doi: 10.1109/TNNLS.2018.2866622.
[59] Q. Zhang, H. Chen, A. A. Heidari, X. Zhao, Y. Xu, P. Wang, Y. Li, and C. Li, "Chaos-induced and mutation-driven schemes boosting salp chains-inspired optimizers," *IEEE Access*, vol. 7, pp. 31243–31261, 2019.
[60] F. Zhang, T. Lei, J. Li, X. Cai, X. Shao, and J. Chang, and F. Tian, "Real-time calibration and registration method for indoor scene with joint depth and color camera," *J. Pattern Recognit. Artif. Intell.*, vol. 32, no. 7, Jul. 2018, Art. no. 1854021.
[61] S. Feng and C. L. P. Chen, "Fuzzy broad learning system: A novel neuro-fuzzy model for regression and classification," *IEEE Trans. Cybern.*, to be published. doi: 10.1109/TCYB.2018.2857815.

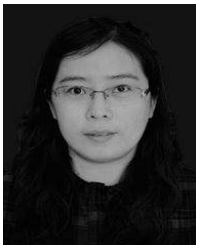

HUIMIN ZHAO (F'77) received the B.S. degree in electrical technology, the M.S. degree in traffic information engineering and control, and the Ph.D. degree in mechanical engineering from Dalian Jiaotong University, Dalian, China, in 2000, 2004, and 2013, respectively. Since 2019, she has been a Professor with the College of Electronic Information and Automation, Civil Aviation University of China, Tianjin, China. Her research interests include artificial intelligence, signal processing, and fault diagnosis.

JIANJIE ZHENG (M'97) received the B.S. degree in software engineering from the Dalian Institute of Science and Technology, Dalian, China, in 2018. He is currently pursuing the master's degree in software engineering with Dalian Jiaotong University, Dalian. His research interests include artificial intelligence and fault diagnosis.

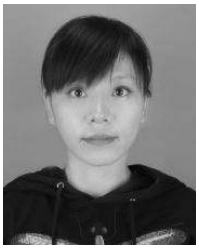

JUNJIE XU (F'85) received the B.S. and M.S. degrees in computer science and technology from Dalian Maritime University, Dalian, China, in 2007 and 2010, respectively, and the Ph.D. degree in computer application technology from Dalian Maritime University, Dalian, in 2016. Since 2016, she has been a Lecturer with the College of Computer Science and Technology, Civil Aviation University of China, Tianjin, China. Her research interests include artificial intelligence and information safety.

WU DENG (M'76) received the B.S. degree in electrical technology and the M.S. degree in computer application technology from Dalian Jiaotong University, Dalian, China, in 2001 and 2006, respectively, and the Ph.D. degree in computer application technology from Dalian Maritime University, Dalian, in 2012. Since 2019, he has been a Professor with the College of Electronic Information and Automation, Civil Aviation University of China, Tianjin, China. His research interests include artificial intelligence, optimization method, and fault diagnosis.